CCAMLR Science, Vol. 18 (2011): 97–122

SENSITIVITY INVESTIGATION OF THE SDWBA ANTARCTIC KRILL TARGET STRENGTH MODEL TO FATNESS, MATERIAL CONTRASTS AND ORIENTATION

L. Calise✉ and G. Skaret
Observation Methodology Group
Institute of Marine Research
PO BOX 1870 Nordnes
N-85817 Bergen
Norway
Email – lucio@imr.no

Abstract

The distorted-wave Born approximation model is recognised as state-of-the-art in predicting acoustic target strength (TS) from fluid-like marine organisms. A stochastic version, the so-called SDWBA model, is endorsed by CCAMLR to predict the TS of Antarctic krill (*Euphausia superba*) for use in the acoustic echo-integration method. In this study, the SDWBA TS pattern and frequency response behaviours at standard survey frequencies and animal lengths are explored via a sensitivity analysis of some important parameters: number of stochastic realisations, the fatness factor, the material contrasts between the organism and the surrounding seawater and the distribution of animal orientations. Due to the high variability of TS to realistic changes in parameters, it is important that the model should be parameterised according to the potential seasonal variability of krill in the area of investigation. In a multifrequency context, the girth–length relationship for the body shape parameterisation can give a high source of uncertainty, and there is an urgent need for development of accurate and standard procedures to measure both the material property contrasts and the orientation at the time and location of the actual survey. Moreover, a number of incongruities within the CCAMLR SDWBA model package are identified and proposed solutions implemented in an improved package.

Keywords: Antarctic krill, multifrequency acoustics, target strength, SDWBA model, frequency response, CCAMLR

Introduction

Although zooplankton are small organisms and their echoes weak, they are discernible scatterers of sound within specific frequency ranges. Acoustic estimates of zooplankton abundance can be made rigorously if the scattering as a function of size and frequency for an individual (i.e. target strength (TS)) is known. TS of an aquatic organism can either be measured directly (*in situ* or *ex situ*) or modelled (Foote, 1991). In the case of zooplankton, due to the complexity of the scattering processes, the acoustical estimates rely on the best aspects of both approaches. In recent decades, large efforts have been undertaken to improve theoretical scattering models for zooplankton organisms (e.g. Stanton et al., 1993, 1998a; Demer and Martin, 1995; McGehee et al., 1998; Stanton and Chu, 2000; Lavery et al., 2002; Demer and Conti, 2003). The scattering from an object is given by its form, size and acoustical impedance contrast. The latter depends on the difference in density and sound speed between the object and the surrounding medium. For weak scatterers with complex shapes, such as zooplankton, problems in prediction may arise from uncertainties and inter-dependence connected to these parameters. Exact solutions can be achieved with analytical restrictions but at the cost of a limited range of applicability and high complexity in the implementation. Therefore, either numerical or empirical approximate models have been preferred, especially for euphausiids (e.g. Kristensen and Dalen, 1986; Cochrane et al., 1991; Stanton et al., 1993, 1996, 1998b; Martin et al., 1996; Demer and Conti, 2005; Lawson et al., 2008).

In the early 1990s, a theoretical approach based on the distorted-wave Born approximation (DWBA) was adapted to predict the acoustical

scattering from an elongated fluid-like organism such as krill (Stanton et al., 1993; Chu et al., 1993). The approach explicitly takes into consideration another fundamental parameter of the scattering process: the orientation. At present, among the physics-based models the DWBA model is recognised as state-of-the-art in predicting TS from fluid-like zooplankton (Stanton and Chu, 2000; Demer and Conti, 2005). The model calculates the coherent summation of scattering from discrete cylinders of varying radius that represent the animal body shape when juxtaposed. Hence, numerical parameters describing the actual shape of the organism have to be introduced in the model as basic parameters. One approach is to describe the animal's body by digitising the main morphological structures in two dimensions. McGehee et al. (1998) proposed a generic Antarctic krill (*Euphausia superba*) shape obtained by digitising a specimen based on an image shot with the animal projected in lateral aspect. The authors found a good fit between the TS predicted from the DWBA model and the directly measured TS at 120 kHz. In a further development of the DWBA with that shape parameterisation, Demer and Conti (2003) introduced a stochastic version (SDWBA) which takes into account the stochastic nature of the krill scattering process due to the along-axis deformation and changes in animal body curvature during swimming. With a successive improvement (Conti and Demer, 2006) the SDWBA parameterisation was then ensured for general utility, taking explicitly into account the effects of the interdependence of the model parameters.

This improved SDWBA model has been endorsed by CCAMLR as the 'Antarctic krill TS model' (SC-CAMLR, 2005), and a package of Matlab scripts titled SDWBApackage20050603 was distributed by the US representatives to CCAMLR Members to be employed as the standard tool for *E. superba* biomass estimation.

Since *E. superba* is recognised as the key organism in the Southern Ocean, an evaluation of the SDWBA model in its implemented form was warranted. Firstly, the implementation of the SDWBApackage20050603 was explored in detail and a number of incongruities, both in setting and implementing processes, were identified. Consequently, solutions to be implemented in a more correct package were proposed and verified. This addressed to evaluate the performance of the SDWBA model by testing the sensitivity of some of its fundamental parameters. The aim of this paper is to illustrate the main features observed during the investigation and to draw the attention of SDWBA model users to the potential uncertainty associated with specific parameters. Thereafter, the package with proposed solutions is denoted as SDWBApackage2010 to differentiate from the SDWBApackage20050603. Both the packages and the proposed solutions are described in detail in Appendix 1 for interested CCAMLR users.

Theory

Morse and Ingard (1968, equation 8.1.20, page 413) introduced a general DWBA formulation that accurately describes the acoustic scattering by weakly scattering bodies with arbitrary size, shape, orientation and material properties close to those of the surrounding medium. The formulation is complicated because it involves an evaluation of the backscattering amplitude expressed by a three-dimensional integral within the volume of the body. Stanton et al. (1993) and Chu et al. (1993) proposed an alternative approach that was easier to calculate but still accurate given certain assumptions. This was explicitly presented in Stanton et al. (1998a) for deformed cylinder shapes. The triple integral can be numerically replaced by a line integral along the cylinder axis if the following assumptions are valid: (i) the animal is elongated and circular in cross-section at every point along a central curve running through its body; (ii) the material properties only vary axially; (iii) the scatterer has material properties that are close to those of the surrounding water and negligible elastic properties, i.e. weakly scattering fluid-like objects. Despite these restrictions, the line integral form of the DWBA appears to be well suited for a wide range of small marine animals such as euphausiids and copepods (Stanton and Chu, 2000), shrimps (Stanton et al., 1996, 1998b), salps (Wiebe et al., 2010), selected species of pelagic swimbladder-less fish in the post-larval stage (Miyashita, 2003) and squid (Lavery et al., 2007). In practice, the formulation involves the integration of a scattering function along the length of the body axis accounting at the same time for the phase shift arising from its deformation due to the curvature and the variations in cross-sectional radius. Thus, the integration is solved if numerical parameters describing the actual shape of the organism are introduced.

Since it is extremely difficult to generate an analytical formulation that fully describes the krill body, two geometrical approaches have been mostly used to parameterise the organism shape as input for the DWBA, both based on a discretised-bent tapered cylinder form: the uniformly bent cylinder idealisation (e.g. Stanton et al., 1998a) and the body reconstruction by digitalisation (e.g. McGehee et al., 1998). In the first case, the krill body is idealised as a smoothly tapered uniformly bent cylinder defined by the krill length and radius of curvature. The cylinders' cross-sectional radius can then be incorporated in the model as a function of the position along the longitudinal axis and the length. Actually, the body of a euphausiid is not entirely uniformly bent. The dorsal line of the cephalothorax is primarily straight while the abdomen is the bent part. However, Lawson et al. (2006) proposed a reasonable approach to properly infer the parameters by using *in situ* observations during the survey. The cylinder governing the generic krill shape is defined by the ratio between length and cross-sectional radius, and the radius of curvature. The first could be determined from samples captured by nets, the second on the basis of observations by video tools. The DWBA with such body parameterisation has been used to develop an inversion protocol in a multifrequency context for estimating the mean length and density of identified krill aggregations along the Western Antarctic Peninsula (Lawson et al., 2008).

A more accurate representation of the krill body can be achieved by discretising the animal's body by digitisation of the main morphological structures in two dimensions (2D). The 2D approach is validated under the DWBA assumption if the animal is circular in cross-section at every point along a central curve. The digitalisation usually involves deriving the outline of the dorsal and ventral animal surfaces from an image of a specimen in the lateral aspect. A centreline can then be generated on the basis of the digitised points so that for each *j*-th discrete body segment the radius a_j and the position vector $\vec{\mathbf{r}}_{pos_j}$ along this line can be computed on the basis of dorsal–ventral pair points. The sets of positions and radii are then designed to reflect the original shape to be modelled by the DWBA as a juxtaposition of discrete cylinders. The scattering form function f_{bs} can be obtained by summing the components of each digitised body segment *j* as a function of the wave incident angle ϕ (i.e. Demer and Conti, 2003):

$$f_{bs_j}(\phi) = \frac{k_1}{4} \int_{\vec{r}_{pos}} a_j \, (\gamma_\kappa - \gamma_\rho) \, e^{-i2\vec{\mathbf{k}}_1 \cdot \vec{\mathbf{r}}_{pos}} \frac{J_1(2k_2 a_j \cos\beta_{tilt})}{\cos\beta_{tilt}} \, d\vec{\mathbf{r}}_{pos} \quad (1)$$

where $k_m = 2\pi f/c_m$ is the wave number in the medium *m* with the subscripts 1 and 2 referring to the surrounding medium and to the fluid-like medium of the zooplankton body respectively, $\gamma_\rho = (\rho_2 - \rho_1)/\rho_2$ with ρ the mass density, $\gamma_\kappa = \left(\rho_1 c_1^2 / \rho_2 c_2^2\right) - 1$ related to the compressibility $\kappa_i = 1/(\rho_i c_i^2)$, $\vec{\mathbf{k}}_1 = k_1 \, [\sin\phi \; 0 \; \cos\phi \;]^T$ is the incidence wave vector, J_1 is the Bessel function of the first kind of order 1, β_{tilt} the local angle of incidence of the *j*-th cylinder calculated along the centreline using a dot product between $\vec{\mathbf{k}}_1$ and the *j*-th local direction of the centreline. The material properties γ_κ and γ_ρ are allowed to vary inside the fluid-like volume. As a good approximation, the density and sound speed contrasts can be held constant over the modelled krill body, so that the processing is simplified. The definitions of $f(\phi)$ and $\vec{\mathbf{k}}_1$ in equation (1) differ from the DWBA formulations initially presented by Stanton et al. (1998a) and McGehee et al. (1998) implying a different view of the results as described in Appendix 1.

By using equation (1) and a digitised shape, McGehee et al. (1998) found a good fit between DWBA predictions and TS measured at 120 kHz in a chilled tank on the living digitised krill for dorsal, ventral and lateral aspects with respect to the transducer. When the animal orientation was away from these aspect angles, the predicted scattering was much lower than the measured (5–20 dB). Demer and Conti (2003) clarified these deviations taking into consideration the stochastic nature of TS from a krill, and incorporated into the model a phase variability term for each discrete cylinder obtained from a number of realisations of a Gaussian distribution. For the uniformly bent cylinder parameterisation, a numerical method to account for the stochastic nature of the scattering process and the mentioned deviations was already presented by Stanton et al. (1998a).

The proposed Demer and Conti (2003) probabilistic DWBA model, the so-called *Stochastic DWBA* or SDWBA, provides probabilities of TS versus all angles of orientation under the assumption that

there is variability in the phases of the contribution from the scattering elements due to: (i) the stochastic scattering process in a field with noise; (ii) the actual krill shape being more complex than the juxtaposed cylinders of varying radius in the model; (iii) the krill when it swims, because the body flexes and the separate contributions to the scattering from the exoskeleton segments, the tail, the antennas, the eyes, as well as its beating pleopods, increase the stochastic nature of the scattering.

The SDWBA form function for the angle of incidence ϕ is obtained by summing the components f_{bs} calculated for each of the N cylinders with a different random phase φ_j:

$$f_{bs}(\phi) = \sum_{j=1}^{N} \left(f_{bs}(\phi) \right)_j \cdot \exp(i\varphi_j) . \quad (2)$$

For each cylinder j along the body, the phase variability is selected from a Gaussian distribution centred at 0 with standard deviation sd_φ. The backscattering cross-section σ_{bs} is obtained by averaging over multiple realisations of the ensemble of phase φ_j with fixed standard deviation sd_φ, and the TS at a specific angle of incidence ϕ is given by:

$$\begin{aligned} TS(\phi) &= 10\log_{10} \sigma_{bs}(\phi) \\ &= 10\log_{10} \left\langle \left| f_{bs}(\phi) \right|^2 \right\rangle_{\varphi}. \end{aligned} \quad (3)$$

In practice, when the operative frequency, length L and the krill body shape are given, sd_φ can be estimated empirically by comparing the SDWBA predictions with experimental measurements.

In order to establish the basic parameterisation of the SDWBA model for *E. superba*, Demer and Conti (2003) referred to the empirical data at 120 kHz obtained by McGehee et al. (1998) and the related DWBA model parameters. For the specific case of an *E. superba* with 'AT' length (from the anterior margin of the eyes to the tip of the telson without the terminal spines) (Morris et al., 1988) of 38.35 mm, McGehee et al. (1998) used as optimal representation 15 digitised points positioned along a body centreline with corresponding radii. This shape representation was then indicated as the 'generic Antarctic krill shape'. It can be scaled to simulate other krill sizes. In the CCAMLR system, the codified Morris et al. (1988) AT length, has been endorsed as a standard measure for *E. superba*.

Demer and Conti (2003) found the best fit by inferring inter-element phase variability φ with Gaussian distribution centred in 0 and standard deviation $\mathrm{sd}_{\varphi_0} = \sqrt{2}/2 = 0.7071$ radians over 100 random realisations. Furthermore, Demer and Conti (2004) estimated that freshly caught animals were 40% fatter than the animals measured by McGehee et al. (1998) which had been starved for six months, and claimed that this should be taken into account in the SDWBA parameterisation.

However, the utility of the SDWBA model using the generic modelled shape for frequencies higher than that used during the McGehee et al. (1998) experiment was not ensured. Conti and Demer (2006) showed that if the same sd_φ is employed for different frequencies, unrealistic off-axis lobes in the TS pattern are found. The SDWBA prediction versus frequency is stable if the number of cylinders N is large relative to the ratio of organism length to the acoustic wavelength. Hence, in order to ensure general utility of the SDWBA model, the effects of the interdependence between the parameterisation factors have to be explicitly taken into account. Since the morphometric complexity of the body causes the frequency-dependence of the scattering, the results in the frequency domain are comparable if the product $f \cdot \mathrm{sd}_\varphi(f)$ is kept constant with reference to the experimental product $f_0 \cdot \mathrm{sd}_{\varphi_0}$. In addition, the spatial resolution of the digitised body shape has to be constant relative to the acoustic wavelength. Hence, the dimensional ratio $L/N\lambda$, with L the length of the animal, N the number of cylinders and λ the wavelength, should be kept equal to the reference experimental ratio $L_0/N_0\lambda_0$ where N_0 is the number of discrete cylinders composing the reference shape. The SDWBA prediction at frequencies f higher than the reference frequency f_0 should therefore be calculated by adjusting N and sd_φ according to Conti and Demer (2006):

$$\begin{aligned} N(f, L) &= N_0 \frac{f}{f_0} \frac{L}{L_0}; \\ \mathrm{s.d.}_\varphi(f, N) &= \mathrm{s.d.}_{\varphi_0} \frac{N_0}{N(f)} \frac{L}{L_0}. \end{aligned} \quad (4)$$

The length ratio in both the equations (4) is used to scale the digitised shape to an arbitrary length L of a krill.

Table 1 lists the model parameters grouped by class relative to their significance for the model with

notations used in the text of this manuscript and in the SDWBApackage20050603 algorithm and their default values. The last parameter describes the orientation of individuals within an aggregation. For a useful quantitative interpretation, the orientation may be modelled as the angle θ in degrees with respect to the horizontal plan. Stanton et al. (1993) demonstrated that the modelling results based on a Gaussian distribution of orientations fit to the measured data when averaging the echoes over a random distribution of scatterers like krill. Thus, the distribution of orientations θ is typically assumed as a Gaussian distribution defined by its mean and standard deviation values ($\theta = N[\overline{\theta}, std\theta]$) in degrees. Inverting the SDWBA model in a least-squares sense over volume backscattering strength measurements at 38 and 120 kHz attributed to krill and net samples from the CCAMLR-2000 Survey data in the Scotia Sea (Hewitt et al., 2002), Conti and Demer (2006) found that the $\theta_0 = N[11°, 4°]$ distribution of orientations gave the best fit to the *in situ* acoustic data. This distribution is adopted by the SDWBApackage20050603 as default. However, studies on krill orientation, using direct observations or inversion techniques, indicate a variety of distributions. The main reported distributions on different species, conditions and methods are given in Table 2. The results are highly variable, mostly because of the different methods of observation and conditions during the investigations. The main differences are between the aquarium and the *in situ* studies, as well as within the latter group on the standard deviation between those inferred from inversions and those directly observed.

Analysis

The performance of the new SDWBApackage2010 was evaluated using sensitivity tests of some parameters with regard to krill length, discrete frequency and fatness factor. The package was run for five krill AT lengths. In addition to the default 38.35 mm, three other lengths (26, 48 and 53 mm) were chosen on the basis of the length-distribution peaks determined within the three clusters of the CCAMLR-2000 Survey (Siegel et al., 2004) to realistically represent the krill size, while the length of 32 mm was included as an intermediate step. Due to the high computational time, the three standard survey frequencies 38, 120 and 200 kHz were used. In addition, 70 and 333 kHz were also used; the first being suggested to be useful in krill studies (SC-CAMLR, 2009, 2010), the second because it was utilised during the Norwegian AKES survey 2008 to the Southern Ocean on board the RV *G.O. Sars* (Wiebe et al., 2010).

Krill fatness changes with season, diet and physiological state. Since the digitised specimens used by McGehee et al. (1998) had been starved for several months, it is reasonable to question if that animal is representative of krill in the wild. In their validation of the SDWBA model to measurements of the total krill TS based on acoustical reverberation in a cavity, Demer and Conti (2004) assumed a 40% increase in fatness of the McGehee et al. (1998) generic krill shape. Although not presented explicitly, such an increment was stated to be more consistent with the measured animals. In the SDWBA model implementation, the increased fatness assumption is achieved by an increment of the girth-to-length ratio, multiplying the radii of the cylinders representing the reference shape by a factor of 1.4. Thereafter, the variable 'fatness' is used with the meaning of girth. Figure 1 shows both the modelled SDWBApackage20050603 and the McGehee et al. (1998) shapes, which are different, as discussed in Appendix 1, with 0 and 40% increase in fatness. If a fatness factor is applied to a modelled shape, an associated increase in body volume is ascribed; this has to be done considering realistic proportions. The most accredited length-to-volume relationship for *E. superba* is the Kils (1979) allometric relationship. For an individual krill of AT length L in mm, the volume V in cm^3 can be estimated by $V = 3.67 \cdot 10^{-6} L^{3.16}$, which for the reference length of 38.35 mm gives a volume of 0.371 cm^3. The total volumes of the SDWBApackage20050603 and the original McGehee et al. (1998) shapes with increasing fatness are presented in Table 3. It must be noted that the shapes do not include pleopods, antennas and some other small body parts. On the other hand, the Kils relationship was determined by aggregating *E. superba* and *Meganyctiphanes norvegica* specimens, with most of the animals (112 out of 190 specimens) of the latter species, which slightly differs in shape from *E. superba*. However, it seems clear that the application of 40% increase in fatness is unrealistic for both shapes. The determined volumes are 0.434 and 0.536 cm^3, which are much higher than the volume estimated by the Kils relationship. The comparison suggests that the application of a fatness coefficient equal to 20 and 15% for the SDWBApackage20050603 and the McGehee et al. (1998) shape respectively is more realistic.

Table 1: Model input parameters grouped by their implication on the SDWBA model and their notation in this paper (Symbol) and SDWBApackage20050603 algorithm.

Class	Parameter	Symbol	Package variable	Unit	Default value	Reference
key	Krill length	L	ActualLength	m	$38.35 \cdot 10^{-3}$	
	Density contrast	g	g0		1.0357	2
	Sound speed contrast	h	h0		1.0279	3
	Seawater sound speed	c	c	m s^{-1}	1456	1
basic	Length	L_0	L0	m	$38.35 \cdot 10^{-3}$	1
	Number of cylinders	N_0	N0		14	1
	Shape	$\vec{\mathbf{r}}_{pos}$, a	r, a	m	Table 3 ref. $1 \cdot 10^{-3}$	1
	Fatness		fatness		1.4	4
	Frequency	f_0	freq0	Hz	$120 \cdot 10^3$	1
	Standard deviation of stochastic phase	sd_{φ_0}	stdphase0	radians	sqrt(2)/2 = 0.7071	4
operational	Incidence angles*	ϕ_i	theta	degrees	–90:269	
	Orientation angles*	θ_i	phi	degrees	90 + theta	
	Frequency range	F	frequency	Hz	$[30:5:200] \cdot 10^3$	
	Stochastic realisations		noise_realisations		100	4
	Scaling factor		scaling		max(r(:,1))/ActualLength	
	Distribution of orientations	θ_0	meanorientation, stdorientation	degrees	N[11,4]	4

References: 1 – McGehee et al. (1998); 2 .– Foote et al. (1990); 3 – Foote (1990); 4 – Conti and Demer (2006). * Note that in all the Demer and Conti works the wave incidence angle is denoted by θ. In this paper the notation ϕ is preferred to avoid misunderstanding with the krill angle of orientation commonly indicated as θ.

Table 2: Summary of relevant published results on distribution of krill orientation N[$\bar{\theta}$,*std*θ] in degrees as defined in the text. The results are based on direct measurements or matching theoretical prediction with acoustic data.

Author(s), year	Species	N[$\bar{\theta}$, *std*θ]	Method
Kils, 1981	*E. superba*	N[45.3,30.4]	Observation in aquarium
	M. norvegica	N[53.8,64.2]	
Kristensen and Dalen, 1986	*M. norvegica*	N[–9.8,34.1]	Observation *in situ* with underwater camera
		N[0,30]	Suggestion of no migratory activity
Cochrane et al., 1991	*M. norvegica*	N[5,5]	Matching by inversion using High-Pass fluid cylinder model prediction with volume backscattering at 50 and 200 kHz.
Endo, 1993	*E. superba*	N[45.6,19.6]	Observation in aquarium
Chu et al., 1993	*E. superba*	N[~20,~20]	Inferred by DWBA model from dual-frequency 38 and 120 kHz, TS data from encaged animals
Miyashita et al., 1996	*E. pacifica*	N[30.4,19.9]	Video observation in small aquarium
Demer and Conti, 2005	*E. superba*	N[15,5]	Matching theoretical prediction by SDWBA model based on biological samples and volume backscattering at 38 and 120 kHz
Conti and Demer, 2006	*E. superba*	N[11,4]	As in Demer and Conti, 2005, with improved parameterization of the SDWBA model
		N[4,2]	
Lawson et al., 2006	*E. superba*	N[0,27]	Direct observations from video plankton recorder

Table 3: SDWBApackage20050603 and digitised McGehee et al. (1998) shape volume for a krill specimen of AT length 38.35 mm applying different fatness factors (increment in girth). The volume is determined by summing the volumes of all cylinders constituting the shape.

Fatness		Volume (cm^3)	
%	factor	SDWBApackage	McGehee et al. (1998)
0	1	0.222	0.273
10	1.1	0.268	0.331
15	1.15	0.293	0.362
20	1.2	0.319	0.394
30	1.3	0.374	0.462
40	1.4	0.434	0.536

In order to investigate the effect of fatness, the model package was also run for each of the chosen lengths with increasing fatness coefficient from 0 to 40% in steps of 10. The first value, which is related to the McGehee et al. (1998) starved animals, was considered as the lower limit and the latter, i.e. the default value for the SDWBApackage20050603, to represent the upper limit for krill.

In addition, the model was configured with the different length–fatness combinations and run with the contrasts g and h determined based on the Chu and Wiebe (2005) length-dependent relationships: $g = 5.439 \times 10^{-4} L + 1.002$ and $h = 4.981 \times 10^{-4} L + 1.009$.

At the end of the multiple runs a database was established to explore the operational parameters. As a first step, it was verified whether the default number of stochastic iterations (100) was appropriate. Both SDWBA packages were run with the number of realisations set to 200, keeping the remaining parameters at the default (Table 1). For each angle of incidence, the backscattering cross-section was averaged over the number of realisations from 25 to 200 in steps of 25. These backscattering patterns and the relative TS predictions determined using equation (3) were then analysed.

Finally, the interdependence between the mean and standard deviation of the Gaussian distribution of orientation was investigated applying the same averaging calculation as implemented in the SDWBApackage20050603 and described in Appendix 1. The predicted σ_{bs} patterns were averaged stepping the mean and the standard deviation over ranges of possible values. A particular focus was made on the association of fatness and four distributions of orientation of *E. superba* in Table 2: the model default N[11°,4°], the Chu et al. (1993) distribution N [20°, 20°], the Conti and Demer (2006) second choice N [4°, 2°] and the proposed Lawson et al. (2006) distribution N [0°, 27°].

Results and discussion

Number of stochastic iterations

For each averaged sigma and TS pattern, the sample variance (dB) around the mean was determined to explore how the number of iterations affected the variability of the results in both the packages. Figure 2 shows the predicted TS variance at 120 kHz when varying the number of stochastic realisations. Although the calculation is an ill-advised process, because performed in the logarithmic domain, it graphically better describes the results derived in linear domain too. In the case of the SDWBApackage20050603, the variance in TS prediction at 120 kHz is stable when increasing the number of realisations above 100. For the SDWBApackage2010, the variance decreases slightly from 100 to 150 realisations and then stabilises. However, for all the investigated realisation steps, the variance is lower for the SDWBApackage2010 than the minimum variance obtained with the SDWBApackage20050603. Similar behaviour was observed for all the investigated frequencies. Despite the slight decrease in variance from 100 to 150 realisations in the SDWBApackage2010, the number of 100 realisations was considered appropriate for practical purposes and used for the further analyses. When running both packages four different times with 100 realisations, the SDWBApackage20050603 TS variances at 120 kHz had a min–max difference of 0.14 compared to 0.07 of the SDWBApackage2010. This indicates that the latter package is less variable not only within a single run but also among different runs. This could be ascribed to the default standard deviation sd_{φ_0} for the inter-element stochastic phase which seems more appropriate for the correct McGehee et al. (1998) modelled krill shape as claimed by Demer and Conti (2003).

Fatness sensitivity

In Appendix 1, the effect of the girth on the predicted TS by using both packages at the reference frequency of 120 kHz is discussed. Figure 3 explicitly shows the effect versus the predicted TS frequency response by using the SDWBApackage2010 for the chosen lengths with default settings but varying the fatness coefficient.

The results demonstrate the strong impact of the girth on TS magnitude, which may introduce high uncertainty in scaling acoustic measurements to estimates of krill biomass. The fatness becomes particularly important at 200 kHz since the TS is weaker for high fatness factors as the length increases. This may influence the analysis of data acquired during surveys where the TS difference between 120 and 200 kHz is often used to discriminate between scatterers or size modes within the same group of organisms.

For AT lengths of 38.35 and 48 mm, weaker TS at 120 than at 200 kHz is predicted at a low fatness factor, but it becomes stronger as the factor increases.

Sections 1 and 2 in Table 4 present the predicted TS levels for both the SDWBApackage20050603 and the SDWBApackage2010. The difference in TS between the packages decreases with increasing frequency. Generally, it also increases as the fatness factor increases, except for 38 kHz where it is stable. However, when comparing the frequency TS pattern versus angle of incidence, the magnitude of the observed differences is reduced as a consequence of averaging over a range of angles (see e.g. Figures A3 and A4).

At 120 kHz the difference in TS levels from low to high fatness factors decreases substantially as the length increases. At 200 kHz, since the distribution of orientations N[11°,4°] does not involve incidence angles outside the main lobe, the weakness in the resampling procedure for the SDWBApackage20050603, described in Appendix 1, is not evident.

In general, all changes in frequency of the distinct TS with fatness seem to be activated relative to the transition region (Rayleigh-Optical regions), which is strictly related to the size of the animal. The fat content of the krill varies between individuals and times, especially related to the feeding supply and maturity stage. Thus, when applying the SDWBA on survey data, knowledge of the girth of net-sampled krill, in addition to length, may help to infer a correct parameterisation of the actual shape and reduce potential sources of high uncertainty. It is also a question whether the increased fatness factor should be applied only to those cylinders representing specific parts of the body where the girth is more important.

Inferring length-dependent material property contrasts

When setting the *g* and *h* contrasts according to the Chu and Wiebe (2005) length-dependent relationships and otherwise default parameterisation, similar trends to those shown in Figure 3 were found, but at different TS levels. Section 3 of Table 4 lists the TS predictions obtained by using the SDWBApackage2010 run for the chosen lengths with default setting, but applying the length-dependent *g* and *h* contrasts and varying the fatness coefficient.

For animals smaller than 48 mm, the TS levels are lower than those obtained with the default fixed contrasts, with deviations notably higher for smaller sizes (up to 3.8 dB for animal length of 26 mm). Generally, this would cause overestimates of the biomass of small krill. Since the krill's acoustic material properties have very strong spatial and temporal variability, the need for more measurements of density and sound–speed contrasts at the location and during the season of the actual survey is clear. Certainly, due to anatomical differences within the krill body, inhomogeneities in material properties are expected; therefore, the basic approximation of constant contrasts over the entire krill body is an initial source of uncertainty. This issue should be further investigated in the future, since there is a general lack of available published data.

Effects averaging the distribution of orientation

Figure 4 illustrates the main features observed exploring the effect on the TS prediction of different combinations of mean standard deviation of the Gaussian distribution of orientation. The results are related to the application of a 20% fatness factor, which appears to be more appropriate than 40% to represent the shape of *E. superba* in the wild. The σ_{bs} patterns were averaged (see Appendix 1) over different mean (0, 10 and 20 degrees) and standard deviation (5, 10, 20 and 30 degrees) of the Gaussian distribution of orientation.

It is observed that when the mean is equal or close to 0°, the relative differences between frequencies are stable but the TS levels are very sensitive to the standard deviation. As the patterns are averaged over a broader distribution of tilt angles (i.e. larger standard deviation) the resulting TS at all the frequencies are lower.

An inverse behaviour is observed as the mean goes away from the range of angles where the TS main lobe is predicted. For the mean close to 10° (second column panels), the TS levels are less sensitive to the standard deviation and the relative differences between frequencies are stable for standard deviation larger than 10°. For a standard deviation of 5° (black line), the TS at higher frequencies has a

Table 4: Predicted SDWBApackage20050603 and SDWBApackage2010 TS (dB re 1 m^2) at standard acoustic frequencies for krill having different AT lengths (L) and fatness (fts) with distribution of orientations θ = N[11°,4°]. The other parameters were set as default (Table 1). Section 3 shows output from runs with length-dependent density contrast (g) and sound speed contrasts (h). Note that 38 mm refers to the AT standard length of 38.35 mm.

L (mm)	fts (%)	SDWBApackage20050603					SDWBApackage2010										
		1. f (kHz)					2. f (kHz)					3. f (kHz)					
		38	70	120	200	333	38	70	120	200	333	g, h	38	70	120	200	333
26	0	–97.1	–88.2	–82.9	–80.0	–77.8	–95.4	–86.7	–82.0	–79.3	–77.4	1.0161	–99.7	–91.0	–86.3	–83.6	–81.7
	10	–95.5	–86.6	–81.6	–79.1	–77.6	–93.8	–85.1	–80.6	–78.4	–77.4	1.0220	–98.0	–89.4	–84.9	–82.7	–81.7
	20	–94.0	–85.2	–80.4	–78.3	–77.6	–92.3	–83.7	–79.5	–77.8	–77.6		–96.5	–88.0	–83.8	–82.1	–82.0
	30	–92.7	–83.9	–79.3	–77.8	–77.7	–91.0	–82.4	–78.4	–77.3	–78.0		–95.2	–86.7	–82.8	–81.6	–82.4
	40	–91.4	–82.7	–78.4	–77.4	–77.9	–89.7	–81.3	–77.6	–77.0	–78.6		–94.0	–85.6	–81.9	–81.4	–83.0
32	0	–92.1	–83.9	–80.1	–76.4	–76.5	–90.4	–82.6	–79.3	–76.3	–76.4	1.0194	–93.4	–85.6	–82.3	–79.3	–79.5
	10	–90.5	–82.5	–78.9	–76.2	–76.8	–88.8	–81.2	–78.0	–75.7	–77.2	1.0249	–91.8	–84.2	–81.1	–78.8	–80.3
	20	–89.0	–81.0	–77.8	–75.7	–77.2	–87.3	–79.8	–77.1	–75.4	–78.2		–90.3	–82.8	–80.1	–78.4	–81.3
	30	–87.6	–79.8	–77.0	–75.4	–77.7	–86.0	–78.6	–76.3	–75.2	–78.9		–89.0	–81.6	–79.4	–78.3	–82.0
	40	–86.4	–78.7	–76.3	–75.3	–78.0	–84.7	–77.5	–75.8	–75.2	–78.8		–87.7	–80.5	–78.8	–78.2	–81.8
38	0	–87.8	–80.7	–77.7	–74.5	–76.9	–86.2	–79.5	–76.6	–74.2	–77.4	1.0229	–88.1	–81.4	–78.5	–76.1	–79.2
	10	–86.2	–79.2	–76.6	–74.3	–77.4	–84.6	–78.1	–75.6	–73.9	–77.7	1.0281	–86.5	–79.9	–77.6	–75.8	–79.6
	20	–84.8	–77.9	–75.9	–74.1	–77.2	–83.2	–76.9	–74.9	–73.9	–77.0		–85.1	–78.8	–76.7	–75.8	–78.9
	30	–83.5	–76.8	–75.2	–74.2	–76.2	–81.9	–75.7	–74.3	–74.0	–75.9		–83.7	–77.6	–76.1	–75.9	–77.8
	40	–82.3	–75.7	–74.6	–74.2	–75.1	–80.6	–74.8	–73.9	–74.2	–75.3		–82.5	–76.7	–75.8	–76.0	–77.1
48	0	–82.8	–77.2	–74.2	–72.7	–75.8	–81.4	–76.3	–73.1	–72.3	–75.2	1.0281	–81.8	–76.6	–73.5	–72.6	–75.5
	10	–81.2	–75.9	–73.4	–72.8	–74.3	–79.7	–75.0	–72.5	–72.5	–74.5	1.0329	–80.1	–75.3	–72.8	–72.8	–74.8
	20	–79.8	–74.8	–72.9	–73.0	–73.4	–78.4	–74.0	–72.1	–73.0	–74.6		–78.8	–74.3	–72.4	–73.2	–74.8
	30	–78.6	–73.7	–72.6	–73.3	–73.4	–77.1	–73.0	–71.8	–73.6	–74.6		–77.5	–73.4	–72.1	–73.8	–74.9
	40	–77.4	–72.9	–72.4	–73.6	–73.5	–76.0	–72.2	–71.8	–74.1	–73.8		–76.3	–72.5	–72.1	–74.4	–74.2
53	0	–80.7	–75.8	–72.8	–72.2	–74.0	–79.3	–75.0	–71.8	–72.0	–74.1	1.0308	–79.0	–74.7	–71.5	–71.6	–73.7
	10	–79.2	–74.6	–72.2	–72.5	–73.2	–77.8	–73.7	–71.3	–72.6	–74.1	1.0354	–77.5	–73.4	–71.0	–72.1	–73.7
	20	–77.8	–73.6	–71.9	–72.9	–73.0	–76.4	–72.8	–71.1	–73.3	–73.8		–76.1	–72.5	–70.7	–72.8	–73.4
	30	–76.6	–72.7	–71.6	–73.3	–72.5	–75.2	–72.0	–71.2	–73.8	–72.9		–74.9	–71.7	–70.9	–73.4	–72.6
	40	–75.4	–72.0	–71.6	–73.5	–71.1	–74.1	–71.4	–71.1	–73.8	–72.7		–73.8	–71.0	–70.7	–73.4	–72.2

distinct response for all the AT krill lengths. While for standard deviations starting from 20°, the levels in TS are similar to those obtained with zero mean for all frequencies. For a mean of 20° (third column panels), the relative differences between frequencies are not stable when setting different standard deviations, with a particular response for the lowest standard deviation (black lines).

In general, for mean orientations ranging from 10° to 20°, the TS levels become stronger as the standard deviation increases in contrast to the zero mean orientation. This is still valid for mean orientation values higher than 20° (not shown in Figure 4). However, with means from 10° to 20°, the TS is still less sensitive to the standard deviation but the dependence increases with higher mean values overall if the standard deviation becomes higher than 15°.

Figure 4 illustrates results for a generic krill shape with fatness increased by 20%. Setting other fatness factors, similar reciprocal features in TS frequency response were observed, apart from the changes discussed in the fatness sensitivity subsection. Figure 5 shows the predicted TS frequency response obtained by running the SDWBApackage2010 with the limits of the fatness factor set to 0 and 40% and averaging the predicted σ_{bs} patterns over the chosen distributions of orientation other than the default. The effects of the fatness on the distinct frequency TS trends are highlighted for the default distribution in Figure 3. They are also shown in Figure 5 for all three distributions. In particular, for the distribution N [4°, 2°] at 120 kHz the change in TS trend with the fatness factor as length increases is visible for a krill length of 53 mm. Despite the Chu et al. (1993) N [20°, 20°] and the Lawson et al. (2006) N [0°, 27°] distributions being markedly different in mean orientation, they are similar in trends and close in TS. Obviously, when both mean and standard deviation lie within the range of the predicted main lobe angles, higher TS is found at lower frequencies, as for the distribution N [4°, 2°].

The results in Figures 4 and 5 clearly indicate that knowledge of the orientation angle distribution of krill during a survey is essential for a proper application of the SDWBA model. High-quality observations of orientation *in situ* are difficult to obtain; however, it seems crucial to develop and routinely apply standard methodologies to measure this parameter during the survey.

Conclusions

Acoustic TS is a stochastic variable and despite the effects of its variability being fairly smoothed when considering integration quantities on large-scale acoustic surveys, the requirement for a well-functioning model predictor is necessary. Correct application of the SDWBA model for krill still needs accurate characterisation of the many parameters. This study demonstrates the implication at the standard survey frequencies for a range of animal sizes. Different basic shape parameterisation and model functions affect the TS predictions.

Firstly, although the high level and the elegance of the SDWBApackage20050603 implementation endorsed by CCAMLR to predict the TS for the *E. superba* was recognised, a number of incongruities have been identified, both in parameter settings and choice of processes. The comparison between the predicted levels of scattering obtained from the current package and from the proposed solutions indicates that the differences are in general not negligible and addressed to investigate the sensitivity of the SDWBA model of some important parameters in general. For the default setting at the reference frequency 120 kHz the TS peak of the main lobe of the improved package is 1.3 dB stronger. However, results have to be interpreted with consideration of the level of accuracy required from a model predictor within the entire process of acoustic krill biomass estimation.

Together with the well-known krill TS model problem due to the correct values of the material properties, this study highlights the strong impact of length–girth ratio parameterisation for the krill shape in the SDWBA model. It has been shown how this source of uncertainty may potentially affect the TS patterns and the analysis in a multifrequency context, reflecting both the process of acoustical to biological conversion and scrutinising krill from other scatterers. It is also a question whether the currently applied parameterisation is biologically realistic. While the material properties contrasts mostly influence the magnitude of the predicted TS levels, the shape parameters delineate the trend in frequency response by shifting the transition region along the frequency range; hence, they indirectly

affect the relative differences between frequencies of the integration quantities which are quantitatively used to estimate the krill biomass.

When applying the SDWBA to acoustic survey data, the model should be parameterised according to the potential seasonal variability of krill present in the study area. In accordance with several other studies and reports, the need to perform accurate measurements of density and sound-speed contrasts and tilt angle, possibly during krill acoustic surveys, is highlighted here. In addition, this study showed that a standard definition of the girth measure to be carried out on net-sampled krill associated with the length measurements is warranted.

It has been shown that the results from the SDWBA model depend strongly on the standard deviation of tilt angle distributions. It is strongly suggested that standard methodologies for measurement of this parameter should be developed and routinely applied during surveys.

Since there is high variability in the output with small changes in single parameters, application of the SDWBA model in automatic system using inversion method techniques should be implemented with care.

Acknowledgement

This work was supported by The Royal Norwegian Ministry of Fisheries and Coastal Affairs through the project 'Antarctic Krill and Ecosystem Studies (AKES)' with additional contributions by the Institute of Marine Research, The University of Bergen, Norwegian Antarctic Research Expeditions, The Research Council of Norway, The Norwegian Petroleum Directorate, Norsk Hydro (StatoilHydro) and ABB Norway, and by The Research Council of Norway through the project 'Exploiting new Wideband Echo Sounder Technology for ZOOplankton characterization, sizing and abundance estimation (WESTZOO)' project no. 190318.

References

Chu, D. and P.H. Wiebe. 2005. Measurements of sound-speed and density contrasts of zooplankton in Antarctic waters. *ICES J. Mar. Sci*., 62 (4): 818–831.

Chu, D., K.G. Foote and T.K. Stanton. 1993. Further analysis of target strength measurements of Antarctic krill at 38 and 120 kHz: comparison with deformed-cylinder model and inference of orientation distribution. *J. Acoust. Soc. Am*., 93 (5): 2985–2988.

Cochrane, N.A., D.D. Sameoto, A.W. Herman and J. Neilson. 1991. Multiple-frequency acoustic backscattering and zooplankton aggregations in the inner Scotian Shelf Basins. *Can. J. Fish. Aquat. Sci*., 48 (3): 340–355.

Conti, S.G. and D.A. Demer. 2006. Improved parameterisation of the SDWBA for estimating krill target strength. *ICES J. Mar. Sci*., 63 (5): 928–935.

Demer, D.A. and L.V. Martin. 1995. Zooplankton target strength: volumetric or areal dependence? *J. Acoust. Soc. Am*., 98 (2): 1111–1118.

Demer, D.A. and S.G. Conti. 2003. Reconciling theoretical versus empirical target strengths of krill: effects of phase variability on the distorted-wave Born approximation. *ICES J. Mar. Sci*., 60 (2): 429–434. (See in addition: Demer and Conti, 2004.)

Demer, D.A. and S.G. Conti. 2004. Erratum – Validation of the stochastic distorted-wave Born approximation model with broad bandwidth total target strength measurements of Antarctic krill. *ICES J. Mar. Sci*., 61 (1): 155–156.

Demer, D.A. and S.G. Conti. 2005. New target-strength model indicates more krill in the Southern Ocean. *ICES J. Mar. Sci*., 62 (1): 25–32.

Endo, Y. 1993. Orientation of Antarctic krill in an aquarium. *Nippon Suisan Gakkaishi*, 59 (3): 465–468.

Foote, K.G. 1990. Speed of sound in *Euphausia superba*. *J. Acoust. Soc. Am*., 87 (4): 1405–1408.

Foote, K.G. 1991. Summary of methods for determining fish target strength at ultrasonic frequencies. *ICES J. Mar. Sci*., 48 (2): 211–217.

Foote, K.G., I. Everson, J.L. Watkins and D.G. Bone. 1990. Target strengths of Antarctic krill (*Euphausia superba*) at 38 and 120 kHz. *J. Acoust. Soc. Am.*, 87 (1): 16–24.

Hewitt, R.P., J.L. Watkins, M. Naganobu, P. Tshernyshkov, A.S. Brierley, D.A. Demer, S. Kasatkina, Y. Takao, C. Goss, A. Malyshko, M.A. Brandon, S. Kawaguchi, V. Siegel, P.N. Trathan, J.H. Emery, I. Everson and D.G.M. Miller. 2002. Setting a precautionary catch limit for Antarctic krill. *Oceanography*, 15 (3): 26–33.

Kils, U. 1979. Preliminary data on volume, density and cross section area of Antarctic krill, *Euphausia superba* – Results of the 2. German Antarctic Expedition 1977/1978. *Meeresforschung*, 27 (3): 207–209.

Kils, U. 1981. The swimming behaviour, swimming performance and energy balance of Antarctic krill *Euphausia superba*. *BIOMASS Sci. Ser.*, 3: 122 pp.

Kristensen, Å. and J. Dalen. 1986. Acoustic estimation of size distribution and abundance of zooplankton. *J. Acoust. Soc. Am.*, 80 (2): 601–611.

Lavery, A.C., T.K. Stanton, D.E. McGehee and D. Chu. 2002. Three-dimensional modeling of acoustic backscattering from fluid-like zooplankton. *J. Acoust. Soc. Am.*, 111 (3): 1197–1210.

Lavery, A.C., P.H. Wiebe, T.K. Stanton, G.L. Lawson, M.C. Benfield and N. Copley. 2007. Determining dominant scatterers of sound in mixed zooplankton populations. *J. Acoust. Soc. Am.*, 122 (6): 3304–3326.

Lawson, G.L., P.H. Wiebe, C.J. Ashjian, D. Chu and T.K. Stanton. 2006. Improved parametrization of Antarctic krill target strength models. *J. Acoust. Soc. Am.*, 119 (1): 232–242.

Lawson, G.L., P.H. Wiebe, T.K. Stanton and C.J. Ashjian. 2008. Euphausiid distribution along the Western Antarctic Peninsula – Part A: Development of robust multi-frequency acoustic techniques to identify euphausiid aggregations and quantify euphausiid size, abundance, and biomass. *Deep-Sea Res. II*, 55 (3–4): 412–431.

McGehee, D.E., R.L. O'Driscoll and L.V. Martin Traykovski. 1998. Effects of orientation on acoustic scattering from Antarctic krill at 120 kHz. *Deep-Sea Res. II*, 45 (7): 1273–1294.

Martin, L.V., T.K. Stanton, P.H. Wiebe and J.F. Lynch. 1996. Acoustic classification of zooplankton. *ICES J. Mar. Sci.*, 53 (2): 217–224.

Miyashita, K. 2003. Diurnal changes in the acoustic-frequency characteristics of Japanese anchovy (*Engraulis japonicus*) post-larvae 'shirasu' inferred from theoretical scattering models. *ICES J. Mar. Sci.*, 60 (3): 532–537.

Miyashita, K., I. Aoki and T. Inagaki. 1996. Swimming behaviour and target strength of isada krill (*Euphausia pacifica*). *ICES J. Mar. Sci.*, 53 (2): 303–308.

Morris, D.J., J.L. Watkins, C. Ricketts, F. Buchholz and J. Priddle. 1988. An assessment of the merits of length and weight measurements of Antarctic krill *Euphausia superba*. *Brit. Ant. Surv. Bull.*, 79: 27–50.

Morse, P.M. and K.U. Ingard. 1968. *Theoretical Acoustics*. Princeton University Press, Princeton, NJ: 927 pp.

SC-CAMLR. 2005. Report of the First Meeting of the Subgroup on Acoustic Survey and Analysis Method (SG-ASAM). In: *Report of the Twenty-fourth Meeting of the Scientific Committee (SC-CAMLR-XXIV)*, Annex 6. CCAMLR, Hobart, Australia: 563–585.

SC-CAMLR. 2009. Report of the Fourth Meeting of the Subgroup on Acoustic Survey and Analysis Methods. In: *Report of the Twenty-eighth Meeting of the Scientific Committee (SC-CAMLR-XXVIII)*, Annex 8. CCAMLR, Hobart, Australia: 473–510.

SC-CAMLR. 2010. Report of the Fifth Meeting of the Subgroup on Acoustic Survey and Analysis Methods. In: *Report of the Twenty-ninth Meeting of the Scientific Committee (SC-CAMLR-XXIX)*, Annex 5. CCAMLR, Hobart, Australia: 147–171.

Siegel, V., S. Kawaguchi, P. Ward, F. Litvinov, V. Sushin, V. Loeb and J. Watkins. 2004. Krill demography and large-scale distribution

in the southwest Atlantic during January/ February 2000. *Deep-Sea Res. II*, 51 (12–13): 1253–1273.

Stanton, T.K. and D. Chu. 2000. Review and recommendations for the modelling of acoustic scattering by fluid-like elongated zooplankton: euphausiids and copepods. *ICES J. Mar. Sci*., 57 (4): 793–807.

Stanton, T.K., D. Chu, P.H. Wiebe and C.S. Clay. 1993. Average echoes from randomly oriented random-length finite cylinders: zooplankton models. *J. Acoust. Soc. Am.*, 94 (6): 3463–3472.

Stanton, T.K., D. Chu, and P.H. Wiebe. 1996. Acoustic scattering characteristics of several zooplankton groups. *ICES J. Mar. Sci*., 53 (2): 289–295.

Stanton, T.K., D. Chu, and P.H. Wiebe. 1998a. Sound scattering by several zooplankton groups. II. Scattering models. *J. Acoust. Soc. Am.*, 103 (1): 236–253.

Stanton, T.K., D. Chu, P.H. Wiebe, L.V. Martin and R.L. Eastwood. 1998b. Sound scattering by several zooplankton groups. I. Experimental determination of dominant scattering mechanisms. *J. Acoust. Soc. Am.*, 103 (1): 225–235.

Wiebe, P.H., D. Chu, S. Kaartvedt, A. Hundt, W. Melle, E. Ona and P. Batta-Lona. 2010. The acoustic properties of *Salpa thompsoni*. *ICES J. Mar. Sci*., 67 (3): 583–593.

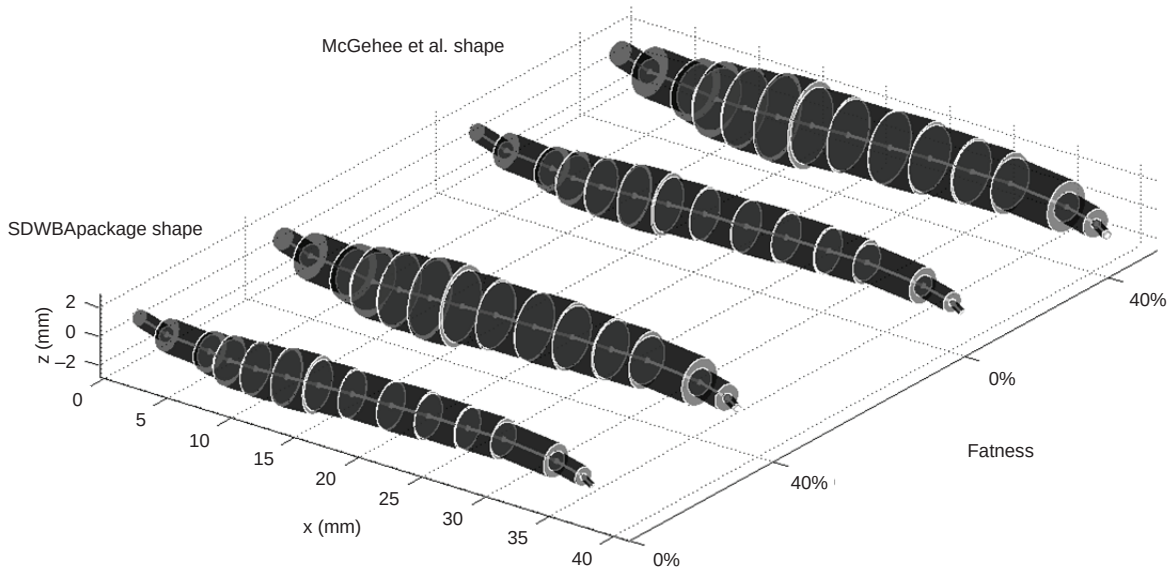

Figure 1: Illustration of the SDWBApackage20050603 shape and the original McGehee et al. (1998) shape (see Table A1), parameterised with 0 and 40% increase in fatness, modelled to determine the SDWBA TS prediction of *Euphausia superba* with standard AT length of 38.35 mm.

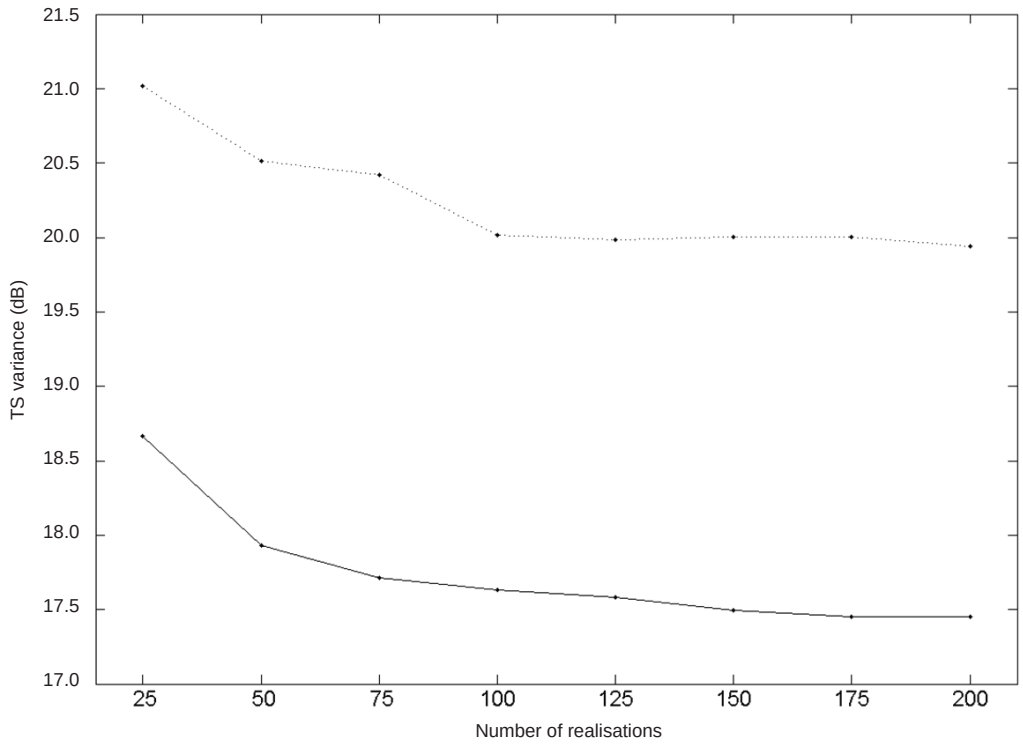

Figure 2: Variance in dB of the averaged TS pattern versus number of stochastic realisations for the SDWBApackage20050603 (dot-dashed line) and the SDWBApackage2010 (dot-solid line) predictions at 120 kHz. All parameters were set with default values as listed in Table 1.

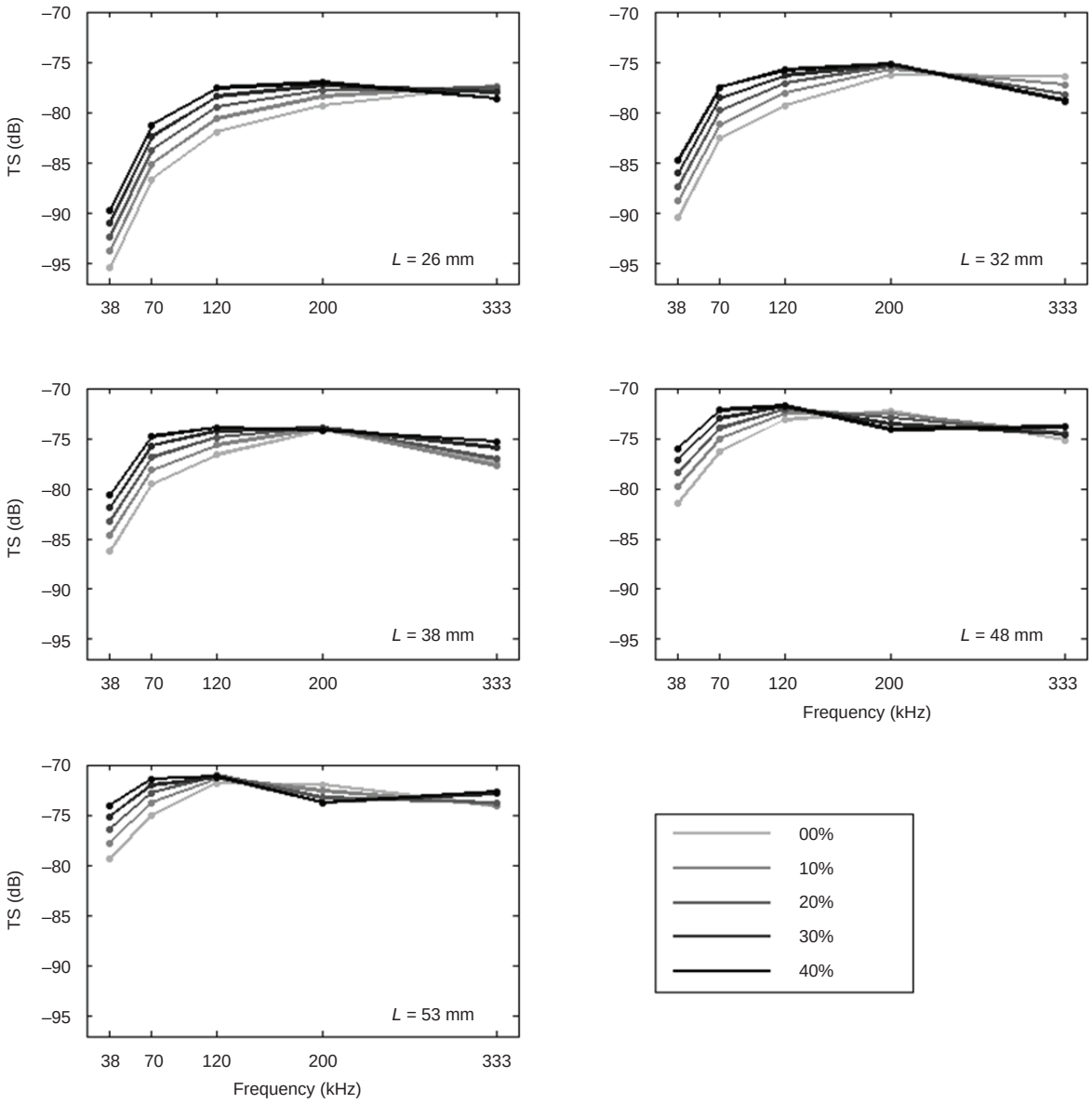

Figure 3: Predicted SDWBApackage2010 TS frequency response (dB re 1 m^2) by using the five common survey frequencies for krill with different AT lengths (L in different panels) and fatness coefficient (grey lines) obtained by averaging σ_{bs} patterns over 100 realisations of the random phase and computed over the distribution of orientations $\theta = N[11°,4°]$. All other parameters were set with default values (Table 1). Note that the 38 mm length is actually referring to the AT standard length of 38.35 mm.

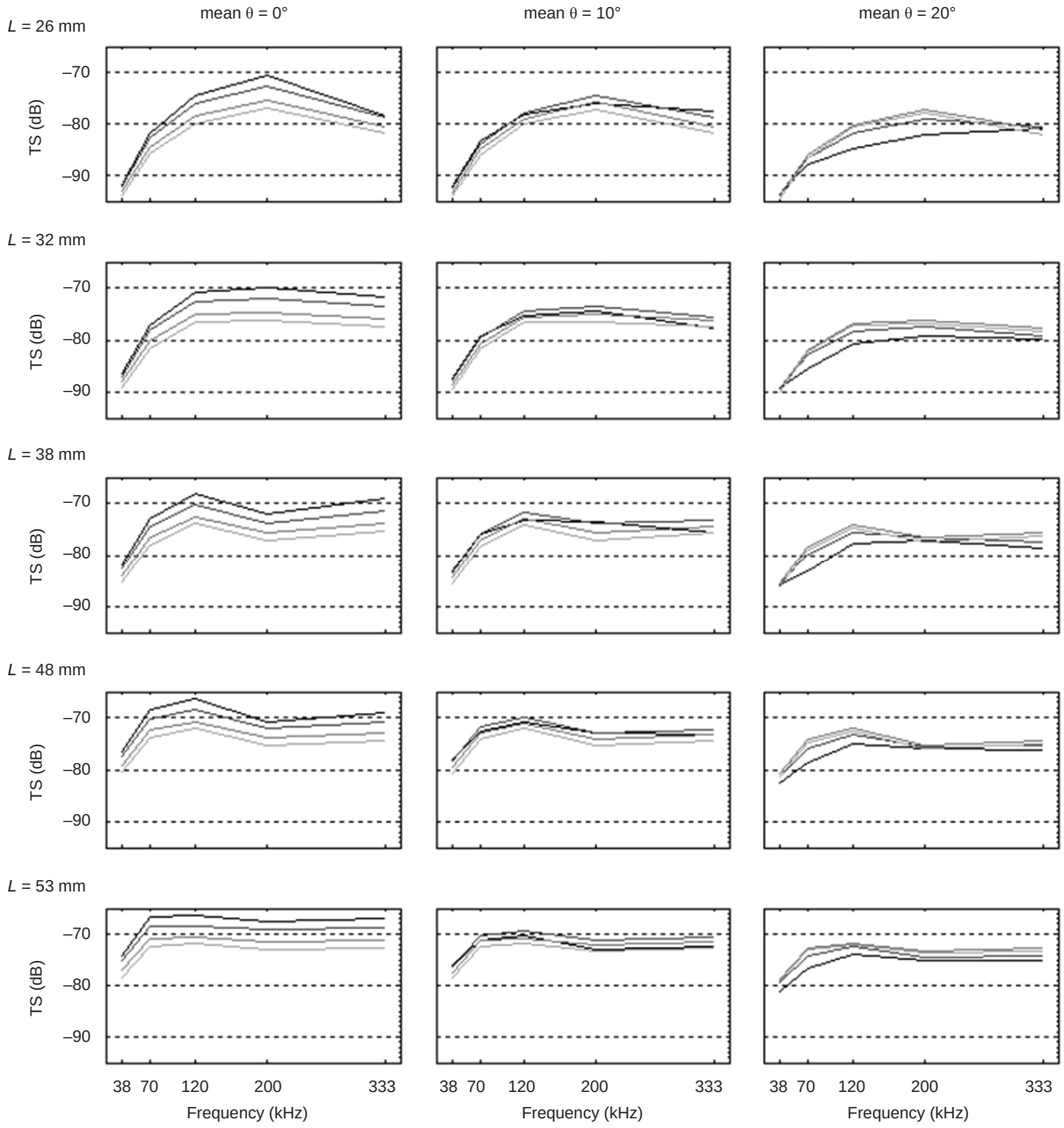

Figure 4: Predicted SDWBApackage2010 TS frequency response (dB re 1 m^2) by using the five common survey frequencies for krill with different AT lengths (L) increased by 20% in fatness and averaging the σ_{bs} patterns over different means (column panels) and standard deviations (5, 10, 20 and 30 degrees, from dark to light) of the Gaussian distribution of orientation. All other parameters were set as default according to Table 1. The 38 mm length refers to the AT standard length of 38.35 mm.

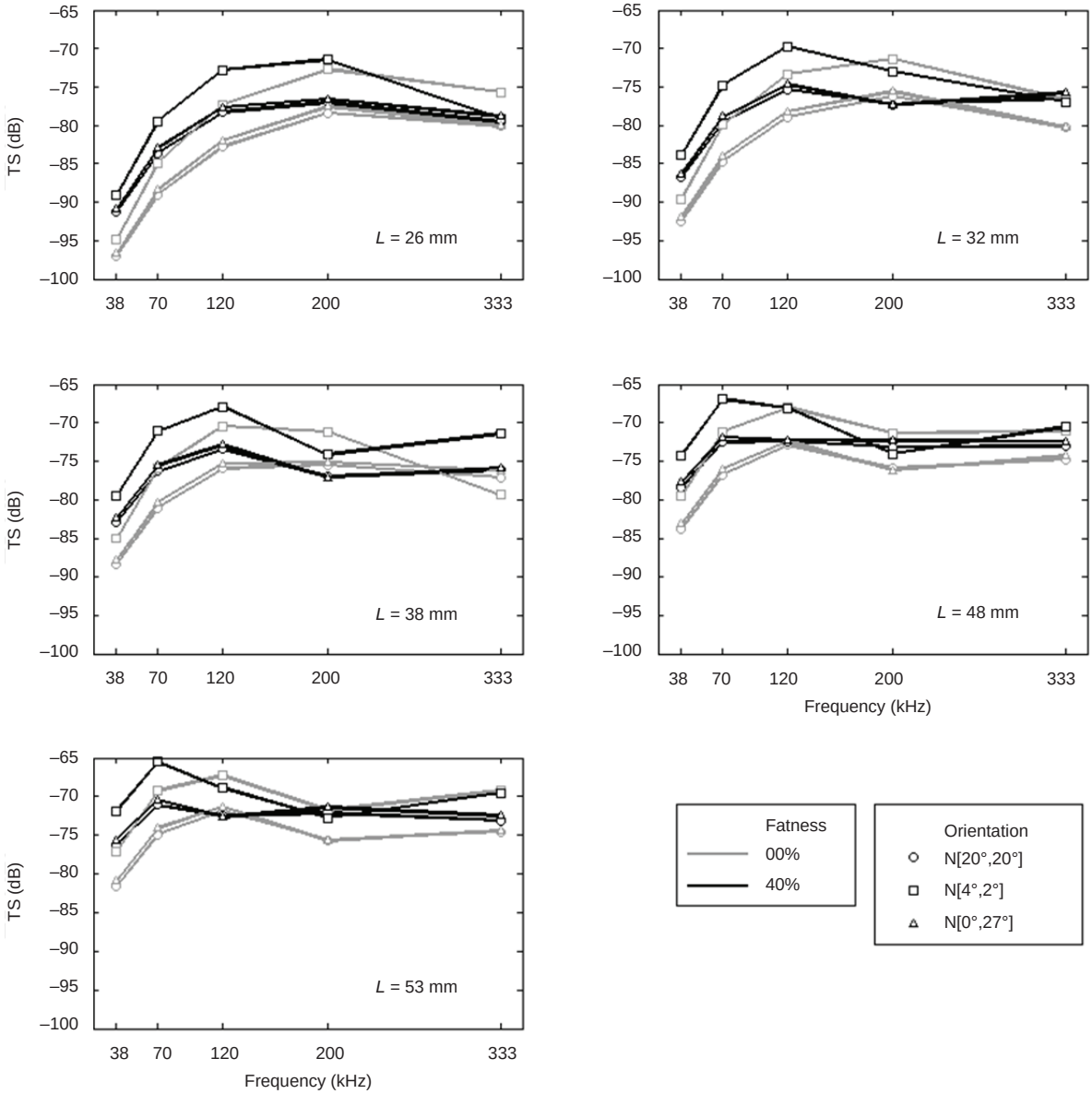

Figure 5: Predicted SDWBApackage2010 TS frequency response (dB re 1 m^2) by using the five common survey frequencies for krill with different AT lengths (L in different panels) with 0 to 40% increases in fatness (grey lines) and averaging the σ_{bs} patterns over three distributions of orientation: the Chu et al. (1993) distribution $N[20°, 20°]$ (circle), the second distribution proposed by Conti and Demer (2006) $N[4°, 2°]$ (squared) and the Lawson et al. (2006) distribution $N[0°, 27°]$ (triangle). All other parameters were set with default values (Table 1). The 38 mm length refers to the AT standard length of 38.35 mm.

Appendix 1

CORRECTIONS TO THE SDWBA MODEL PACKAGE ENDORSED BY CCAMLR

The SDWBA model package endorsed by CCAMLR to predict target strength (TS) from Antarctic krill (*Euphausia superba*) is the SDWBApackage20050603 implemented by Dr S. Conti and distributed by Dr D. Demer (USA) to CCAMLR Members after the 2005 SG-ASAM meeting. The package comprises a number of Matlab scripts and estimates the TS for a krill with arbitrary length over a given range of angles of incidence. Formally, the algorithm follows that presented in McGehee et al. (1998, Appendix A), but includes the phase variability realisations to take into account the stochastic nature of the scattering process (Demer and Conti, 2003) and a resampling process on the shape describing the krill body (Conti and Demer, 2006) as indicated by equations (4).

In addition, the package can average the TS over a given distribution of orientation versus frequency and determine coefficients of a polynomial representation of that function, the so-called 'simplified SDWBA'. The examination of these implementations was not the scope of this study.

The package comprises one main script and eight functions. The main script 'ProcessKrill EsupSDWBATS.m' provides two processing options: calculate the TS or average the TS over a distribution of orientation. In the first case, the parameters of the model can be changed from the default values (Table 1). When all parameters are chosen, for each of the stochastic realisations the script determines the frequency function of TS over the given range of angle orientation by using the functions 'BSTS_SDWBA.m' and 'DWBA_integrandBS.m'. In contrast with the algorithm presented by McGehee et al. (1998), the BSTS_SDWBA.m calculates the backscattering TS using the angle of incidence ϕ as azimuth. This is done on the basis of $f(\phi)$ and $\vec{\mathbf{k}}_1$ definitions in equation (1) and calculating the TS for the angle of orientation θ (= 90 + ϕ) after a proper conversion of $\vec{\mathbf{k}}_1$ (line 95) and calculation of β_{tilt} (line 107). As a result, when the body digitalisation is performed on a 'head left view' image and the model processing starts from the cylinder representing the telson, the dorsal aspect of the animal corresponds to a 90° incident angle while the McGehee et al. (1998) implementation used 270°.

The SDWBApackage20050603 was verified with regard to the basic parameters and algorithmic solutions. The examination revealed three main incongruities: (i) incorrect position vector $\vec{\mathbf{r}}_{pos}$ and ensemble of radii a values delineating the shape of the standard generic krill as defined by McGehee et al. (1998); (ii) incorrect reference length applied when scaling krill with lengths different from the basic krill AT length L_0 = 38.35 mm; (iii) inappropriate resampling function of the position vector $\vec{\mathbf{r}}_{pos}$ adopted for frequencies higher than the reference f_0 = 120 kHz. All incongruities were resolved by some changes within the existing model framework to realise an improved package used in this study (the SDWBApackage2010).

Shape of the generic *Euphausia superba*

The position vector $\vec{\mathbf{r}}_{pos}$ and the ensemble of radii a delineating the shape of the standard generic krill as defined by McGehee et al. (1998) were incorrectly introduced in the SDWBApackage20050603. This seems to originate from a misunderstanding of the measured 38.35 mm AT length (denoted 'L' in SC-CAMLR (2005), paragraph 11(i)), with the maximum digitised values in the x-dimension of the $\vec{\mathbf{r}}_{pos}$ vector, i.e. the digitised length equal to 41.09 mm ('l' in SC-CAMLR (2005), paragraph 11(ii)). The digitised shape comprises the different body parts which contribute to the scattering, whereas the AT length omits the part from the front of the eye to the joint where the peduncle of the first antenna ends. The digitised length and not the AT length should define the dimension of the juxtaposed cylinders used in the model, however, the SDWBApackage20050603 appears to scale the shape to reach the maximum x-dimension value equal to the AT length. The difference in shape is clear when comparing Figure 7 in McGehee et al. (1998) and Figure 1 in Conti and Demer (2006) (note that the two figures have different projection plans). The 15 positions and

Table A1: The positions (*x*, *y* and *z*) and the radii (*a*) values in mm delineating the krill shape adopted by the SDWBApackage20050603, and those presented in McGehee et al. (1998, Table 3) as generic shape for an *Euphausia superba* of 38.35 mm AT measured length.

Point	SDWBApackage20050603				McGehee et al. (1998)			
	x	*y*	*z*	*a*	*x*	*y*	*z*	*a*
1	38.3500	0	0	0	41.0898	0	0	0
2	36.8563	0.9149	0	0.2147	39.4844	0.9869	0	0.2332
3	34.0464	1.7924	0	0.6525	36.4767	1.9244	0	0.6996
4	29.4160	2.4552	0	1.1296	31.5116	2.6381	0	1.2174
5	26.6247	2.4365	0	1.3537	28.5230	2.6165	0	1.4550
6	23.5253	2.4552	0	1.4470	25.2043	2.6375	0	1.5557
7	20.6967	2.3059	0	1.5964	22.1774	2.4691	0	1.7105
8	17.7000	2.2498	0	1.5497	18.9680	2.4145	0	1.6630
9	15.1888	2.0538	0	1.6524	16.2722	2.2034	0	1.7714
10	12.8456	1.8484	0	1.9044	13.7607	1.9890	0	2.0400
11	10.5304	1.6897	0	1.7551	11.2867	1.8110	0	1.8838
12	8.4672	1.6897	0	1.6524	9.0740	1.8127	0	1.7703
13	6.6468	2.0631	0	1.3816	7.1265	2.2155	0	1.4823
14	2.9687	2.4739	0	1.1016	3.1881	2.6530	0	1.1851
15	0	3.5568	0	0.5508	0	3.8150	0	0.5946

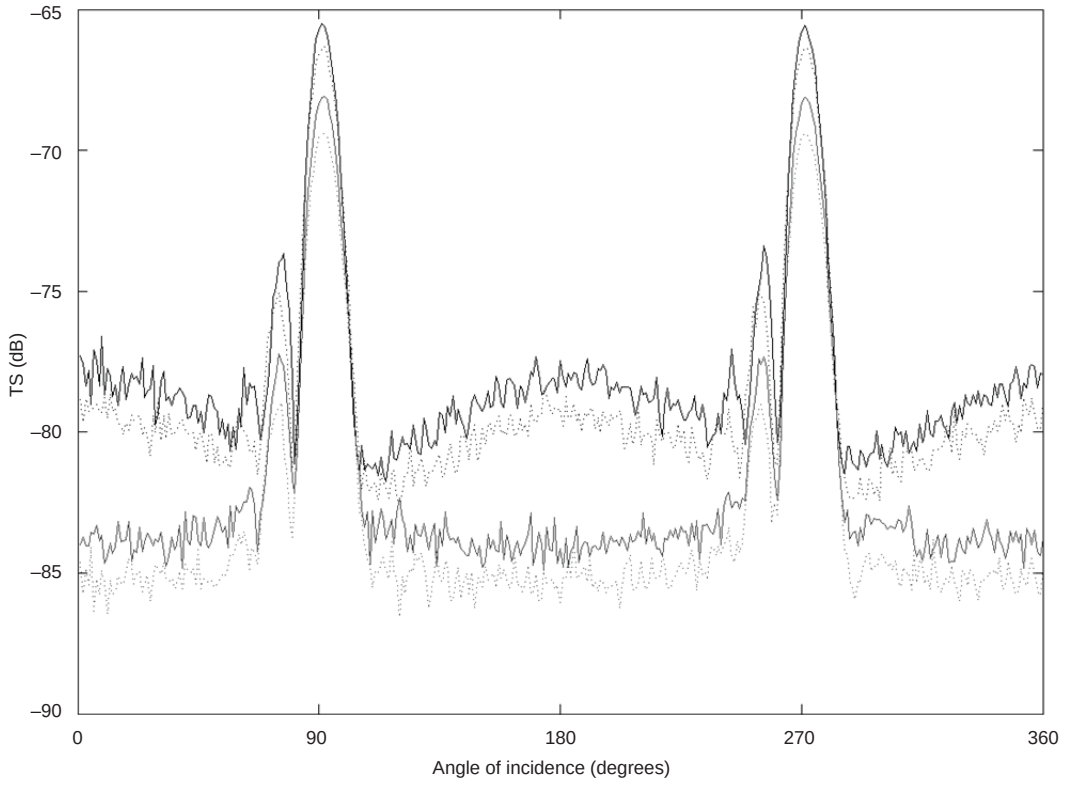

Figure A1: Predicted SDWBApackage20050603 (dashed lines) and SDWBApackage2010 (solid lines) 120 kHz TS patterns (dB re 1 m^2) versus angle of incidence for a krill with AT standard length of 38.35 mm with 0% (grey lines) and 40% (black lines) increased fatness. All the other parameters were set as default according to Table 1.

radii values delineating the shape used in the SDWBApackage20050603 and the original McGehee et al. (1998) shape are listed in Table A1; the difference in length is 7%. The SDWBApackage2010 correctly uses the McGehee et al. (1998) values.

In the comparison of TS predictions between the two packages for the reference frequency 120 kHz and standard settings, the SDWBApackage2010 estimates higher TS at all angles of incidence (Figure A1). This was expected since a shape with longer digitised length is used. The peaks of the first main lobe for 0 and 40% increased fatness were 1.32 and 0.8 dB higher for the SDWBApackage2010 (–68.1 and –65.51 dB versus –69.42 and –66.31 dB). The high relevance of the fatness coefficient for TS prediction in both packages is also evident in both the peak TS levels of the main lobes and the levels and behaviour outside the main lobes. The peak at broadside incidence increases by 3.1 dB for the SDWBApackage20050603 and 2.6 dB for the SDWBApackage2010 when increasing the fatness from 0 to 40%. Outside the main lobes, the pattern assumes a 'parabolic' trend with higher levels around 180° as the fatness increases.

Scaling factor

The SDWBApackage20050603 adopts a scaling process over the standard shape if an AT length other than 38.35 mm is applied as input. The scaling factor is determined using the maximum in the x-dimension of the digitised shape as reference, i.e. the digitised length, rather than the measured AT length, (script 'ProcessKrillEsupSDWBATS.m', line 76). Since the digitised and measured lengths are implemented as equal values in the SDWBApackage20050603, an animal with measured AT length of 38.35 mm would be scaled with a factor equal to 1 (i.e. no scaling but erroneous digitised shape). If the shape is replaced by the original McGehee et al. (1998), the same measured length input (input variable 'ActualLength' = $38.35 \cdot 10^{-3}$ m) will be scaled according to a digitised length of 41.09 mm (Table A1) applying a scaling factor of 1.0714, hence reducing the correct McGehee et al. (1998) shape by 6.7% in length. Since the AT length and the McGehee et al. (1998) shape have been endorsed by CCAMLR as standard, the scaling factor should refer to the basic length L_0. After the introduction of the correct McGehee et al. (1998) shape, the misconstruction can be solved by calculating the scaling factor based on the standard length $38.35 \cdot 10^{-3}$ m, and line 76 in the script 'ProcessKrillEsupSDWBATS.m' should be revised as:

$$\text{scaling} = 38.35 \cdot 1\text{e}{-3}/\text{ActualLength} \tag{A1}$$

Definition (A1) was imposed in the SDWBApackage2010 for this study. It is applicable when the McGehee et al. (1998) shape is used as a basic reference. If another shape is used as reference, the numerator of the definition (A1) has to be substituted by the measured AT length L_0 of the digitised animal.

Resampling process

With the parameterisation given in Conti and Demer (2006), equations (4) have to be formally applied for frequencies higher than the reference $f_0 = 120$ kHz. Within the SDWBApackage20050603, the first of equations (4) is achieved by determining new values for the reference $\vec{\mathbf{r}}_{pos}$ vector and radii through a resampling process using the MatLab Signal Processing Toolbox function 'resample.m' (script 'BSTS_SDWBA.m', lines 67–92). The function uses a polyphase implementation and applies a low-pass anti-aliasing Finite Impulse Response filter (least square linear-phase FIR) to re-characterise the shape through $N(f, L)+1$ position points and radii. The chosen resampling function generates points that do not lie along the original central body line of the digitised krill. This results in artefacts of the modelled shape. Figure A2 shows the 25 points in the x-y plane required to satisfy the first of equations (4) at 200 kHz resulting from the resampling process performed over the 15 reference $\vec{\mathbf{r}}_{pos}$ points representing the SDWBApackage20050603 shape (first two columns in Table A1). The resampled length is greater than the reference length of 38.35 mm whereas these lengths should be equal. The second point of the resampled $\vec{\mathbf{r}}_{pos}$ has coordinates [x = 42.03, y = 0.49] and the last point [x = –0.21, y = 2.32]. When the McGehee et al. (1998) shape with digitised length of 41.09 mm is resampled, the points are [x = 45.03, y = 0.53] and [x = –0.23, y = 3.50] respectively. The consequence of the deviation from the centreline is a shape partly composed of cylinders orientated

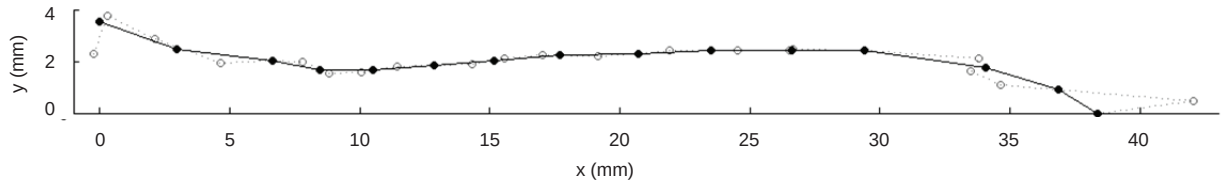

Figure A2: x-y plane body central line of the generic krill shape proposed by McGehee et al. (1998) with standard AT length of 38.35 mm before (black colour line and 15 dots) and after (grey dashed line and 25 open circles) the SDWBApackage20050603 resampling process that generates the shape with 24 cylinders at 200 kHz.

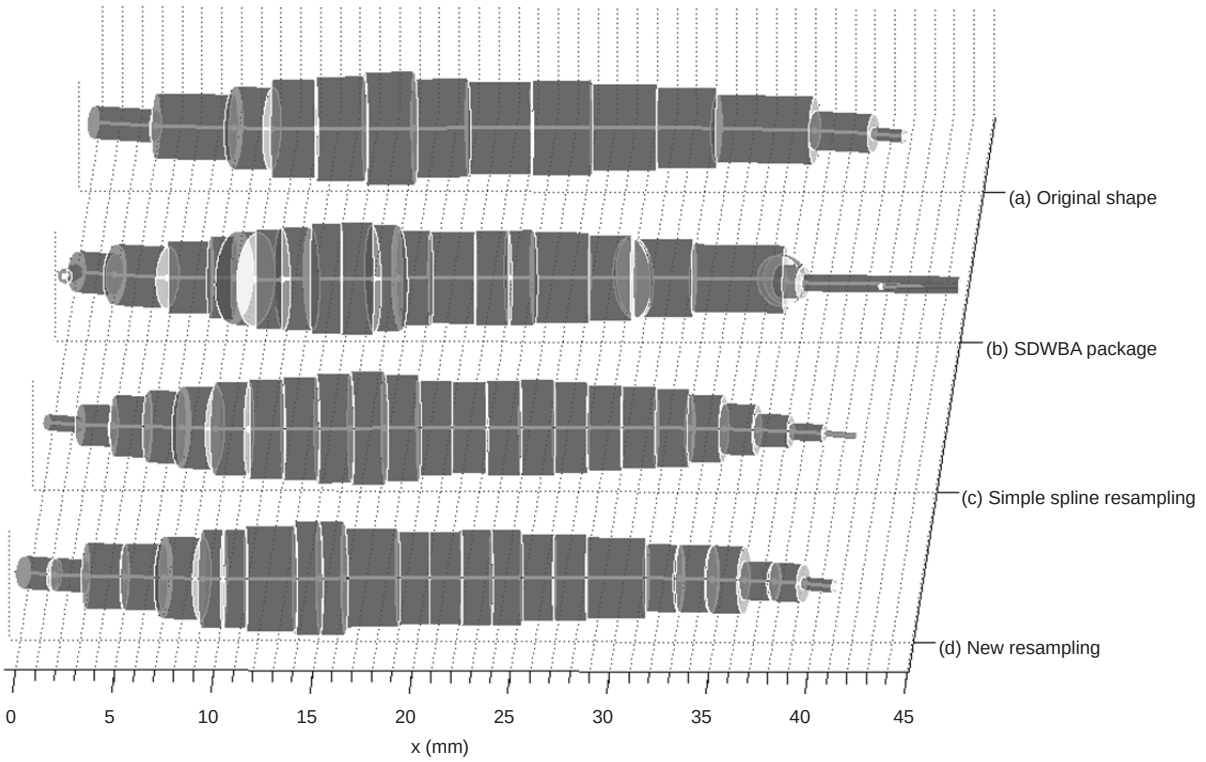

Figure A3: Modelled McGehee et al. (1998) krill shape composed of 14 cylinders with 40% increase in fatness (a) after different resampling processes at frequency 200 kHz (24 cylinders); (b) the SDWBApackage20050603 resampled shape; (c) the simple spline resampled shape proposed in SC-CAMLR (2010); (d) the shape resulting from the proposed resampling and implemented in the SDWBApackage2010.

with unnatural directions. Since the applied resample function is deterministic, krill with a length different from the standard 38.35 mm will have a form that is identical to that unnatural shape, with just the scaling being different. This is also the case for the correct McGehee et al. (1998) shape as illustrated in Figure A3.

As a first approximation, the application of a cubic spline interpolation on the position vector, retaining the resample.m function for the radii values, was suggested to provide an improved characterisation of krill shape (SC-CAMLR, 2010). However, since all the cylinders comprising the shape have almost equal length (Figure A3 plot (c)), the original shape is not fully preserved, as required for a correct comparison of the TS versus frequency results (SC-CAMLR, 2005; Conti and Demer, 2006). Hence, an improved resampling procedure was implemented in the SDWBApackage2010 via the following steps: a uniformly spaced sequence of $N + 1$ points, with N calculated by the first of equations (4), along the digitised length in the x-dimension (from the tale to the head) is generated. Then, each of the generated x-points is replaced by the nearest of the 15 x-values composing the reference generic shape. For each of the 14 generic shape x-intervals the values of the obtained sequence lying within its x-interval are shifted to be equally spaced with respect to the related limits (the original x-values shape). In this way, an x-dimension decreasing

sequence composed of the shifted points and the original shape x-values is obtained. The y-values relative to the new x-sequence is estimated by cubic spline interpolation, so that the x-y points lie along the centreline. Finally, for each point position the associated ray is set equal to that of the original cylinder where the point lies. With such a process, the original shape is perfectly preserved in all its elements, the required number of cylinders is achieved and each cylinder comprising the original shape is subdivided in almost equal parts. Plot (d) in Figure A3 shows the result obtained for the 200 kHz frequency. It can be noted that some of the original cylinders remained unaltered after the resampling, compromising the dimensional requirement between the spatial resolution and the wavelength of the acoustic wave. This happens when no x-value of the initial equally spaced sequence lies within the original x-interval of the unaltered cylinder. However, this artefact vanishes as the frequency increases because the distance between the values of the uniformly spaced sequence decreases and all of the original cylinders have points lying within their x-interval limits. It has been verified that for the McGehee et al. (1998) shape this happens at the frequency of 270 kHz, where 32 cylinders are required by the first of equations (4) and the uniformly spaced sequence is generated by using 1.28 mm step intervals.

Moreover, the proposed resampling might activate the facet effect at the transitions between cylinders of different radii. If this happens, it is more likely to be important at higher frequencies where the wave lengths are smaller than the jump in radius. It is difficult to evaluate this bias but it is reasonable to assume that it is reduced when averaging over a distribution of angle of orientation and/or length.

The new resampling process is validated by calculating the volume of the resulting shapes. The resampled shape has the same volume in cm^3 as the original shape, independent of the frequency, while the SDWBApackage20050603 resampled shape and the simple cubic spline shape volumes vary with frequency. For the McGehee et al. (1998) shape with 40% increase in fatness, the SDWBApackage20050603 increases the volume at frequencies up to 400 kHz and then becomes almost stable, while in the cubic spline process the volume decreases almost linearly as the frequency increases. For instance, the shapes for 200 kHz in Figure A3 plots (a) to (d) have volumes of 0.536, 0.543, 0.533 and 0.536 cm^3 respectively.

Figure A4 shows the predicted 200 and 333 kHz TS patterns versus angle of incidence for a krill with default AT standard length of 38.35 mm and different fatness factors for both the packages. By using equations (4), the number of cylinders was determined as 24 and 39 and the sd of the inter-element phase variability as 0.41248 and 0.25383 radians for 200 and 333 kHz respectively. The dashed lines in the upper panels represent the patterns obtained at 200 kHz without any resampling (i.e. no application of equations 4) to confirm the need of the process for the default digitised shape at frequencies above 120 kHz. It is firstly observed that the SDWBApackage2010 removes the high TS levels at incidence angles just outside the main scattering lobes as predicted by the SDWBApackage20050603. At 200 kHz, the outside main lobe pattern assumes a 'parabolic' trend with peak TS level close to the values of the nearly stable plateau obtained with the SDWBApackage20050603. The plateau with relatively strong and realistically stable TS levels at incidence angles of about 140°–215°, 0°–39°, 320°–360° (Figure A4, upper left panel) may be the effect of the inappropriate resampling process which causes artefacts in the modelled shape of a krill (Figure A3, plot (b)). Conti and Demer (2006) claimed that the obtained frequency-independent plateau was the effect of the corrected adjustment of sd_φ. However, the pattern outside the main scattering lobes for the SDWBApackage20050603 at 333 kHz does not show a stable plateau but distinctly variable TS levels. On the contrary, a plateau appears in the pattern obtained with the SDWBApackage2010, validating the new resampling process. The parabolic trend at 200 kHz in the upper left panel of Figure A4 may be ascribed to the original cylinders that remain unaltered after the resampling (Figure A3, plot (d)) and dominate the scattering process at such angles of incidence. Also for the frequencies 200 and 333 kHz, the influence of the fatness factor on the TS levels is relevant, but with different effects on the main lobe peak than for the reference frequency, especially at 200 kHz. The predictions outside the main scattering lobes follow the expected relative levels, i.e. stronger for higher fatness factor, while within the main lobe an opposite trend is observed. The predicted main lobe peaks at 200 kHz with increased fatness of 0, 20 and 40% are –66, –67.5 and –71 dB respectively for the SDWBApackage20050603 and –65.9, –68.5 and –71.8 (at 98°) for the SDWBApackage2010. The differences in TS levels between the packages over the main lobe are less

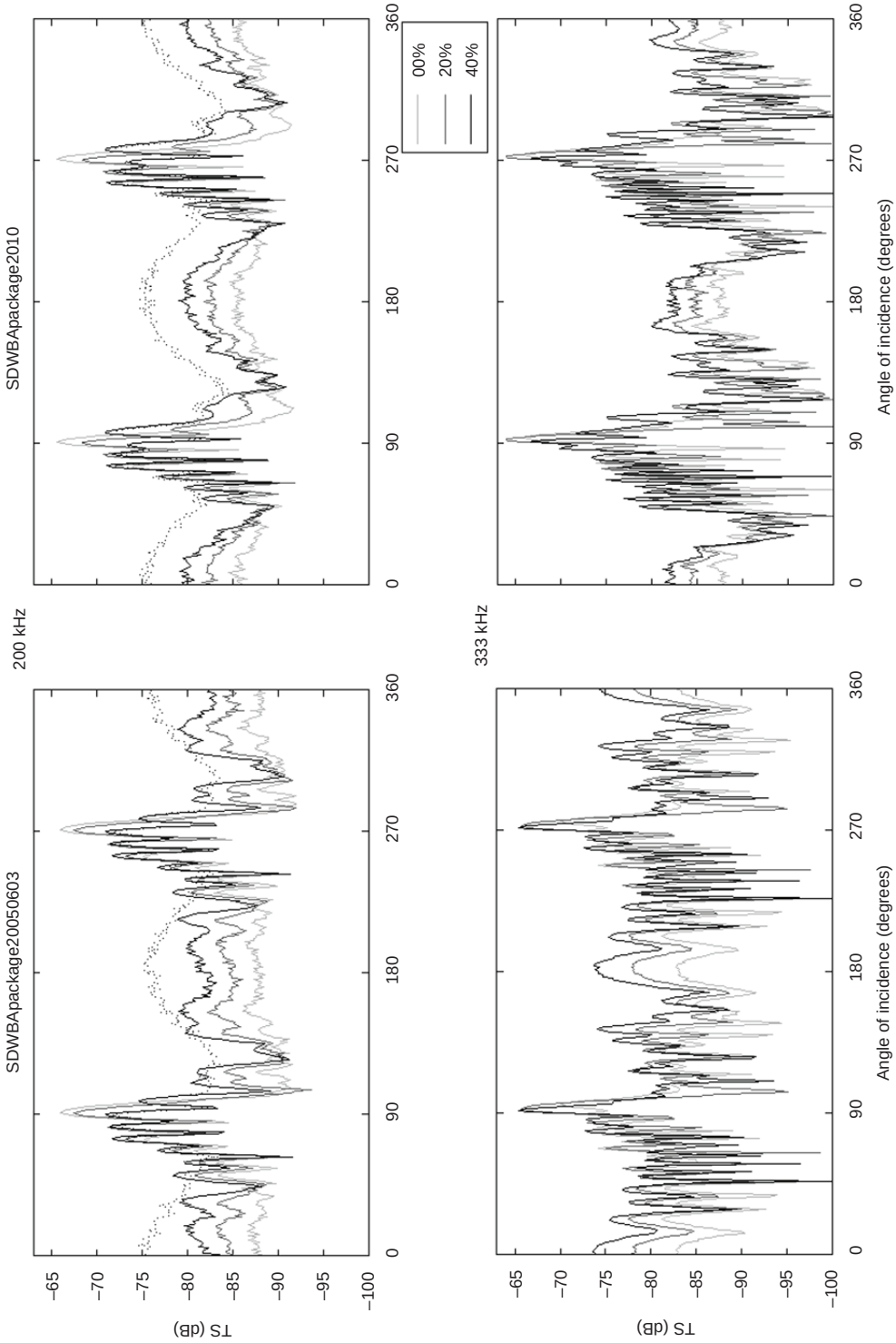

Figure A4: Predicted SDWBApackage20050603 (left panels) and the SDWBApackage2010 (right panels) 200 and 333 kHz TS patterns (dB re 1 m^2) versus angle of incidence for a krill with AT standard length of 38.35 mm and different fatness factors in % (grey lines). All other parameters were set with default values listed in Table 1. The dashed lines plotted for the 200 kHz panels represent the patterns obtained without resampling (i.e. no application of equations (4), N = 14 and $sd_\varphi = 0.7071$).

pronounced for 200 and 333 kHz than for 120 kHz (Figure A1). However, this is not unexpected since the size of the resampled shape is scaled up within the SDWBApackage20050603, reducing the difference in length between the modelled shapes of the packages (Figure A3).

At the end of the TS calculation process, the setting parameters are saved as numbered .mat files in a folder called 'dataSDWBA' (lines 91–94). Further, the mean of the frequency backscattering cross-section for each of the defined angles of orientation over the number of realisations is determined, and consequently the backscattering TS(*f*) by equation (3). These results are saved in a .mat file under a specified filename and folder to be used for the orientation distribution averaging process.

Auxiliary processes within SDWBApackage20050603

Averaging TS over a distribution of orientation

When the second option of the script 'ProcessKrillEsupSDWBATS.m' is chosen, the backscattering cross sections are averaged over a defined Gaussian distribution of orientations $\theta_0 = \mathrm{N}\left[\overline{\theta}_0, std\theta_0\right]$ for each frequency. The script firstly executes this operation running the function 'GaussianOrientation.m' which defines a wrap (the package variable called 'orientation') around the Gaussian distribution for the range of orientations θ_i previously set whereas the backscattering cross sections were calculated:

$$orientation = \frac{A}{\sum A \cdot mean(\Delta\theta_i)}$$

$$\text{with } A = \exp\left(\frac{-(\theta_i - \overline{\theta}_0)^2}{\frac{2}{(std\theta_0)^2}}\right) + \exp\left(\frac{-(\theta_i + 360 - \overline{\theta}_0)^2}{\frac{2}{(std\theta_0)^2}}\right) + \exp\left(\frac{-(\theta_i - 360 - \overline{\theta}_0)^2}{\frac{2}{(std\theta_0)^2}}\right);$$

then, by running the function 'AverageTSorientation.m' to determine the set of σ_{bs} versus frequency as:

$$\sigma_{bs}(f) = \sum_i \sigma_{bs_i}(f) \cdot orientation \cdot mean(\Delta\theta_i). \tag{A1}$$

After averaging over a defined distribution of orientations, a .mat file is saved with a specified orientation filename, including the results and the characteristics of the used distribution.

Simplified SDWBA

Demer and Conti (2005) indicated that the SDWBA TS prediction over a definite distribution of orientations can be simplified as a function of the product of the acoustic wave number *k* and the mean length *L* of the animals under investigation. The function TS(*kL*) can be concisely expressed by a polynomial representation with coefficients estimated over the specific animal orientation distribution. The polynomial order is arbitrary; however, Demer and Conti (2005) stated that a sixth-order polynomial is enough for the purpose and expressed the relationship in the form:

$$\mathrm{TS}(kL) = \mathrm{A}\left(\frac{\log_{10}(\mathrm{B}kL)}{\mathrm{B}kL}\right)^{\mathrm{C}} + \mathrm{D}(kL)^6 + \mathrm{E}(kL)^5 + \mathrm{F}(kL)^4 +$$

$$+ \mathrm{G}(kL)^3 + \mathrm{H}(kL)^2 + \mathrm{I}(kL) + \mathrm{J} + 20 \cdot \log_{10}\left(\frac{L}{L_0}\right). \tag{A2}$$

The SDWBApackage20050603 uses the sixth order as default; however, different orders can be set. The determination of the coefficients and a graphical visualisation of the simplified TS versus frequency are directly obtained by choosing the second option of the main script 'ProcessKrillEsupSDWBATS.m'.

The first term of equation (A2) reflects the non-linear behaviour of the prediction and is found by estimating the three coefficients (*A, B* and *C*) of a non-linear regression using a least-square Gauss-Newton estimation approach through the Matlab function 'nlinfit.m' (script 'SDWBATSfunctioncoeff.m', lines 22–26). A fourth coefficient is also estimated; it is used to determine the coefficient *J* in equation (A2) by summing it with the last of the seven coefficients found by a polynomial curve fitting to the TS predictions in the least-squares sense (script 'SDWBATSfunctioncoeff.m', lines 30–32). The other six polynomial coefficients estimated by the fitting are the function coefficients from *D* to *I* in equation (A2). The last term is for an animal with AT standard length other than the reference $L_0 = 38.35$ mm.

As output, the script 'SDWBATSfunctioncoeff.m' also provides an estimation of the TS error between the simplified model and the SDWBA TS vector versus original *kL* values. This is firstly calculated in the linear domain and then converted to the dB domain (lines 33–41). The mean error can be reduced by increasing the order of the polynomial representation (c.f. Conti and Demer, 2006).

In both SC-CAMLR (2005) and Conti and Demer (2006), the coefficients of the simplified SDWBA model for the reference length $L_0 = 38.35$ mm averaged over the default distribution orientations N [11°, 4°] were presented. The necessary imaginary parts of the coefficients *A, B* and *C* were not included. They can be found in SC-CAMLR (2009, Table 3.1). Also, these imaginary parts do not appear when the coefficients are shown up in the Matlab Command Window during the processing of the 'ProcessKrillEsupSDWBATS.m'. However they are preserved in the variable named 'A' within the Matlab session.